Nanoelectronics and Its New Materials – A NEW ERA OF NANOSCIENCE

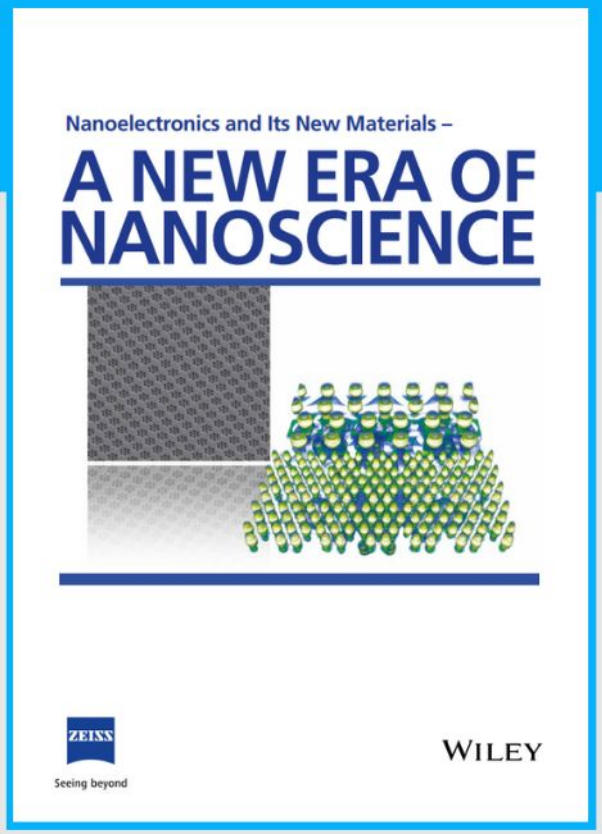

Discover the recent advances in electronics research and fundamental nanoscience.

Nanotechnology has become the driving force behind breakthroughs in engineering, materials science, physics, chemistry, and biological sciences. In this compendium, we delve into a wide range of novel applications that highlight recent advances in electronics research and fundamental nanoscience. From surface analysis and defect detection to tailored optical functionality and transparent nanowire electrodes, this eBook covers key topics that will revolutionize the future of electronics.

To get your hands on this valuable resource and unleash the power of nanotechnology, simply download the eBook now. Stay ahead of the curve and embrace the future of electronics with nanoscience as your guide.

ZEISS

Seeing beyond

WILEY

NANO · MICRO small
www.small-journal.com

Tunable Multicolor Lanthanide Supramolecular Assemblies with White Light Emission Confined by Cucurbituril[7]

*Wei-Lei Zhou, Wenjing Lin, Yong Chen, Xian-Yin Dai, and Yu Liu**

Macrocyclic confinement-induced supramolecular luminescence materials have important application value in the fields of bio-sensing, cell imaging, and information anti-counterfeiting. Herein, a tunable multicolor lanthanide supramolecular assembly with white light emission is reported, which is constructed by co-assembly of cucurbit[7]uril (CB[7]) encapsulating naphthylimidazolium dicarboxylic acid (G_1)/Ln (Eu^{3+}/Tb^{3+}) complex and carbon quantum dots (CD). Benefiting from the macrocyclic confinement effect of CB[7], the supramolecular assembly not only extends the fluorescence intensity of the lanthanide complex G_1/Tb^{3+} by 36 times, but also increases the quantum yield by 28 times and the fluorescence lifetime by 12 times. Furthermore, the CB[7]/G_1/Ln assembly can further co-assemble with CD and diarylethene derivatives (DAE) to realize the intelligently-regulated full-color spectrum including white light, which results from the competitive encapsulation of adamantylamine and CB[7], the change of pH, and photochromic DAE. The multi-level logic gate based on lanthanide supramolecular assembly is successfully applied in anti-counterfeiting system and information storage, providing an effective method for the research of new luminescent intelligent materials.

1. Introduction

Supramolecular intelligent lanthanide luminescence is a research hotspot, owing that the rich energy levels of lanthanide ions and the transitions between different energy levels make them exhibit some unique properties[1] compared with general fluorescent groups, such as long excited state lifetime, large Stokes shift, narrow emission peak width, and high luminous efficiency. Taking advantage of antenna effect,[2] supramolecular capturing light could adequately excite a variety of rare-earth ions (such as Eu^{3+}: red emission, Tb^{3+}: green emission) by energy transfer (ET), achieving full-color fluorescence emission including white light. Therefore, the non-covalent coordination lanthanide supramolecular system can reverse luminescence on/off in response to various stimuli, which has considerable application prospects in optical devices,[3] light-emitting diodes,[4] bio-imaging,[5] information security[6] and full-color displays.[7] For example, Holten-Andersen et al.[8] constructed a multicolor luminescent gel across the white light region through the coordination of terpyridine-terminated four-arm poly(ethylene glycol) with different proportions of Tb^{3+}/Eu^{3+} ions and showed a reversible response to mechano-, vapo-, thermo-, and chemochromism. Li and Zhao et al.[9] reported a printable photo-luminescent supramolecular security material prepared from *bis*-2,6-pyridinedicarboxylic acid/Ln (Eu^{3+} and Tb^{3+}) complex interacting with cationic diarylethene derivative (DAE) via electrostatic interaction. Chen et al.[10] reported a multicolor supramolecular polymer hydrogel with orthogonal adjustability, self-healing, and remodeling ability based on naphthalimide derivatives and acrylamide modified pyridine Tb^{3+}/Eu^{3+} complexes. With the rapid development of lanthanide supramolecular system, the non-covalent polymerization of macrocyclic compounds with lanthanide complex has also received much attention,[11] which can not only improve the ET efficiency,[12] but also introduce functional groups to regulate the luminescence behavior of lanthanide.[13] For instance, we reported a [2]pseudorotaxane from an unsymmetrical diarylperfluorocyclopentene and the complex of Eu^{3+} with terpyridinyldibenzo-24-crown-8 revealing excellent reversible dual-modulated lanthanide-luminescence behavior by host–guest competitive bonding of secondary ammonium salt and K^+ as well as alternating vis/UV irradiation.[14] The lanthanide luminescent assembly of anthracene-bridged *bis*(24-crown-8)terpyridine derivative could not only be reversibly controlled depending on the photoreaction of anthracene unit upon light irradiation or heating, but also shield the quenching of lanthanide luminescence by coordination of 24-crown-8 with alkali or alkaline earth metals.[15] Moreover, the rare-earth up-conversion nanoparticles could excite the phosphorescence emission of cucurbituril/bromophenylpyridinium/hyaluronic acid ternary

W.-L. Zhou, W. Lin, Y. Chen, X.-Y. Dai, Y. Liu
College of Chemistry, State Key Laboratory of Elemento-Organic Chemistry
Nankai University
Tianjin 300071, P. R. China
E-mail: yuliu@nankai.edu.cn
W.-L. Zhou
College of Chemistry and Material Science, Innovation Team of Optical Functional Molecular Devices
Inner Mongolia Minzu University
Tongliao 028000, P. R. China

The ORCID identification number(s) for the author(s) of this article can be found under https://doi.org/10.1002/smll.202304009

DOI: 10.1002/smll.202304009

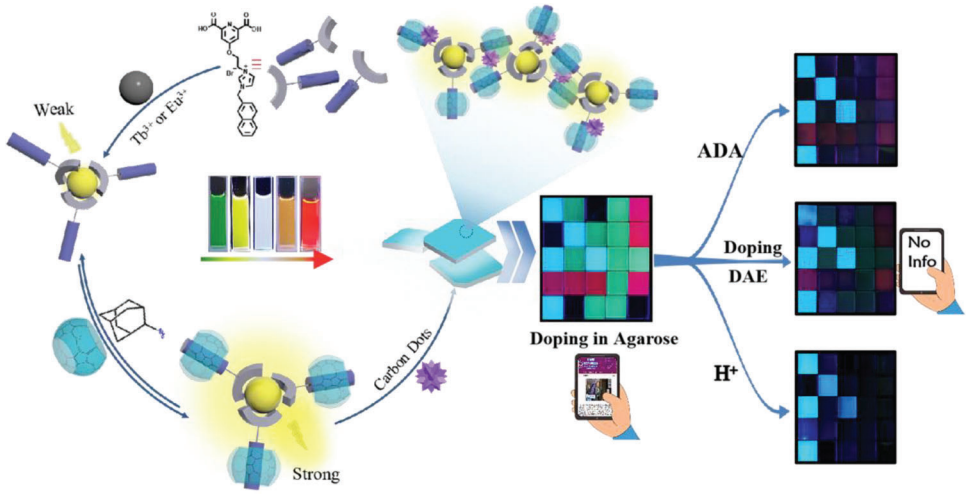

Scheme 1. Schematic illustration of the full-color lanthanide supramolecular assemblies with multiple stimuli responsive.

supramolecular assembly in the near-infrared region, which was successfully applied to targeted cell imaging.[16] However, there are few reports on tight inclusion confinement of CB[7] to achieve panchromatic enhanced and controlled luminescence of rare-earth including white light emission, especially for the construction of multiple logic gates and the application of anti-counterfeiting materials.

Herein, we present a full-color lanthanide luminescent supramolecular assembly in aqueous solution based on the co-assembly of CB[7]/naphthylimidazolium salt of pyridine-2,6-dicarboxylic acid (G_1)/Ln (Eu^{3+}/Tb^{3+}) complexes and carbon quantum dots (CD) (**Scheme 1**). First, the pyridine-2,6-dicarboxylic acid part of G_1 in aqueous solution could coordinate with Ln (Eu^{3+} or Tb^{3+}) in a ratio of 3:1 to form a red or green luminescent complex. Due to the confinement effect of the hydrophobic cavity of CB[7] on the naphthalene imidazolium salt group in G_1, a rotaxane complex with enhanced luminescence was formed along with the quantum yield and fluorescence lifetime of Tb^{3+} increased by 28 times and 12 times, respectively. Whereas for Eu^{3+}, the lifetime increased by 1.1 times and the yield increased by 1.8 times. Based on the trichromatic (RGB) principle, a full-color luminescence spectrum including white light emission with the corresponding CIE (0.31, 0.33) could be achieved, which resulted from the co-assembly of CB[7]/G_1/Ln and CD with superior blue emission by adjusting the ratio of Eu^{3+}, Tb^{3+}, and CD. It is well known that adamantylamine (ADA) is an ideal competitive guest for CB[7]-based complexes. After the addition of the competing guest ADA, the disassembly of CB[7]/G_1/Ln leads to the weakening of lanthanide luminescence in aqueous solution, simultaneously the coordination and dissociation of G_1 controlled by pH (H^+/OH^-), as well as the photoresponse ET between the open/closed-ring and Ln ions after the doping of the DAEs, which all could result in the reversible regulation of the full-color lanthanide luminescent supramolecular assembly CB[7]/G_1/Ln/CD. In addition, using different excitation wavelengths can make the assembly emit different light. Consequently, full-color lanthanide supramolecular assemblies with multiple stimulus responses (competitive bonding, pH, optical, and different excitation wavelengths) were constructed successfully and applied to multi-level logic gates anti-counterfeiting materials.

2. Results and Discussion

The lanthanide-pseudo[2]rotaxane complex was constructed by CB[7] and naphthylimidazolium salt of pyridine-2,6-dicarboxylic acid (G_1) coordination with lanthanide ions in Scheme 1. The ligand G_1 was synthesized (Figures S1–S3, Supporting Information) according to reported method,[17] and the structure was presented in Scheme S1, Supporting Information. Similar to previous work, CB[7] could form a highly stable 1:1 complex with naphthylpyridinium. First, the optical property and host–guest binding behavior of CB[7] with G_1 were explored by the UV–vis absorption and fluorescence emission (**Figure 1**a,b). The band at 250–300 nm was assigned to the absorption of naphthalene, and the emission at 330 nm was the characteristic emission peak of naphthalene. Upon the addition of CB[7] into the aqueous solution of G_1, the bands at 220 nm and 250–300 nm gradually decreased along with appearance of one apparent isosbestic point at 230 nm in the UV–vis spectrum (Figure 1a), and the emission at 330 nm increased continuously,[16] (Figure 1b) which was attributed to the strong host–guest interaction between naphthylimidazolium salt and CB[7] limiting the molecular rotation of the guest G_1 and reducing the non-radiative transition. These phenomena indicated that G_1 was inside the CB[7] cavity. Accordingly, the association constant (K_a) between G_1 and CB[7] was calculated to be $K_a = 9.08 \times 10^5$ M^{-1} at 25 °C by analyzing the sequential changes in UV–vis spectra (ΔA) of G_1 at varying concentrations of CB[7] using a nonlinear least-squares curve-fitting method according to literature reports (Figure S4a, Supporting Information). The Job's plot gave an inflection point at a molar ratio of 0.5, corresponding to a 1:1 host–guest inclusion stoichiometry, which was consistent with the previously reported result. To further prove the inclusion, ^{1}H NMR spectra (Figure S5, Supporting Information) showed that the naphthylimidazolium protons shifted upfield upon complexation with CB[7]. In addition, pyridine-2,6-dicarboxylate (DPA) could form stable compounds with high association constants with lanthanide ions

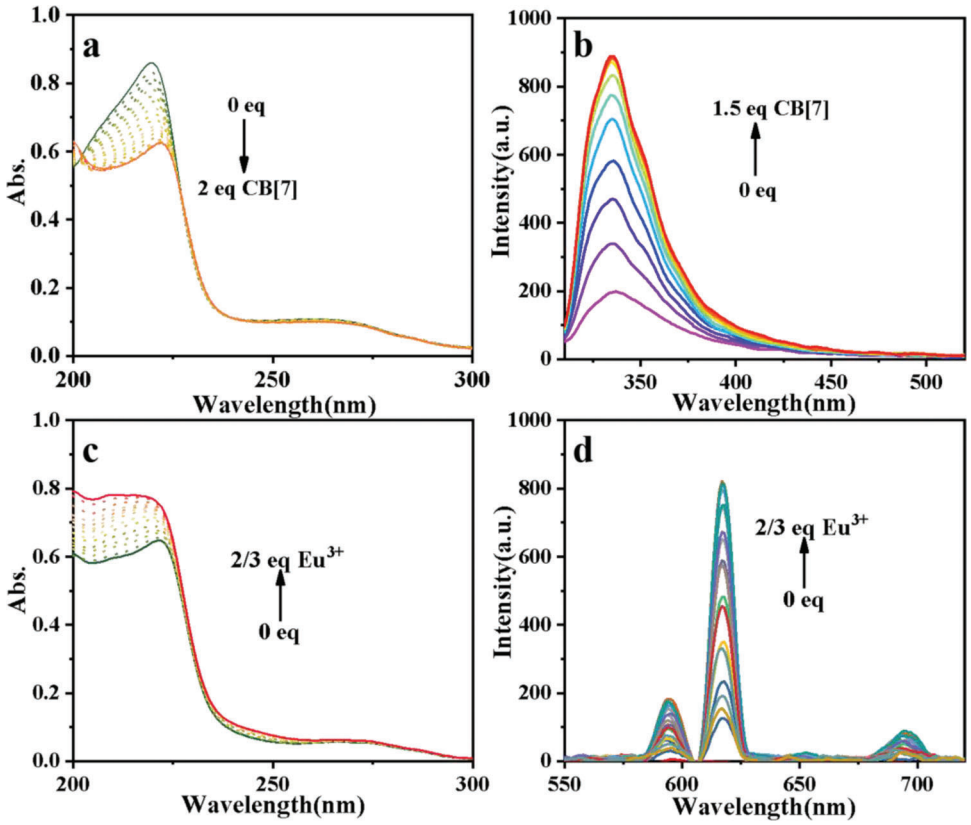

Figure 1. a) Absorption spectra of 0.01 mM G_1 with 2 eq CB[7] and b) emission spectra of 0.01 mM G_1 with 1.5 eq CB[7] in water at 25 °C. c) Absorption spectra and d) emission spectra of 0.01 mM CB[7]/G_1 with 2/3 eq Eu^{3+} in water at 25 °C.

(Tb^{3+}/Eu^{3+}).[6,11] Then we studied the optical properties of lanthanide coordination by UV–vis spectroscopy and fluorescence spectroscopy respectively. Figure 1c shows the increase of the absorption at 250 nm after the addition Eu^{3+} ion (2/3 eq) into ligand CB[7]/G_1 solution (CB[7] = [G_1] = 0.01 mM), along with the emergence of four sharp emission peaks at 590 nm ($^5D_0 \rightarrow {}^7F_1$), 615 nm ($^5D_0 \rightarrow {}^7F_2$), 645 nm ($^5D_0 \rightarrow {}^7F_3$) and 680 nm ($^5D_0 \rightarrow {}^7F_4$) in Figure 1d, which account for an ET process from DPA to Eu^{3+}. The stoichiometry ratio for the complexation of Eu^{3+} ion with G_1 was investigated by the fluorescence spectral titration experiment, and the stoichiometric ratio was measured as 1:3 between Eu^{3+} and G_1 from the curve of ΔF (complex-induced changes of fluorescence intensity at 615 nm) versus [Eu^{3+}]/[G_1] molar ratio in Figure S6, Supporting Information. In addition, the gradual addition of Tb^{3+} ion to the assembly CB[7]/G_1 led to the characteristic emission peak 490 nm ($^5D_4 \rightarrow {}^7F_6$), 545 nm ($^5D_4 \rightarrow {}^7F_5$), 583 nm ($^5D_4 \rightarrow {}^7F_4$), and 621 nm ($^5D_4 \rightarrow {}^7F_3$) of Tb^{3+} in the fluorescence spectrum.

It is worth noting that the CB[7]/G_1/Ln pseudorotaxane lanthanide complex has a significant improvement in optical properties compared with that of G_1/Ln. For Tb^{3+}, the luminescence intensity is enhanced by 36 times, the quantum yield is increased by 28 times, and the lifetime is increased by 12 times, as shown in **Figure 2**a,c, Figures S7a,b and S8a,b, Supporting Information. For Eu^{3+}, the luminescence intensity is enhanced by 1.8 times, the quantum yield is increased by 1.8 times, and the lifetime is increased by 1.1 times (Figure 2b,d, Figures S7c,d and S8c,d, Supporting Information). According to previous reports, this phenomenon may be due to the confinement of the macrocycle to prevent the rotation of the molecule and reduce the energy loss of the ligand molecule, as well as the formed assembly also reducing the coordination number of H_2O. The water coordination number (q) of Ln in the assembly before and after the addition of CB[7] was also calculated according to the lifetime and the reported method[6e,17] (Figure S9 and Table S1, Supporting Information). The q value in the G_1/Tb^{3+} aqueous solution was about 1.95, while the q value of the assembly CB[7]/G_1/Tb^{3+} was reduced to 0.38. This result indicates that the addition of CB[7] not only has a confined effect on G_1 to reduce the non-radiative transition, but also effectively shields the coordination of water molecules with Ln to a certain extent, increases the sensitization of the antenna molecule G_1,[12,17] and then promotes the luminescence behavior of Ln. Furthermore, we compared the morphology, particle size, and potential of the assemblies. The morphology of assembly was observed by transmission electron microscopy (TEM) (Figure S10, Supporting Information) where the morphology of G_1, CB[7]/G_1, and CB[7]/G_1/Tb^{3+} were changed from needle-like nanofibers (50 nm), nanoparticles (200 nm) to the larger nanoparticles (300 nm). Meanwhile, the dynamic light scattering (DLS) test showed the corresponding hydrodynamic radius (Rh) as 263, 313, and 448 nm, which is basically consistent with the TEM results (Figure S11, Supporting Information). Moreover, the zeta potentials of G_1, G_1/Tb^{3+}, and CB[7]/G_1/Tb^{3+} ranged from −8.03, −4.04 to 0.72 mV, indicating that the

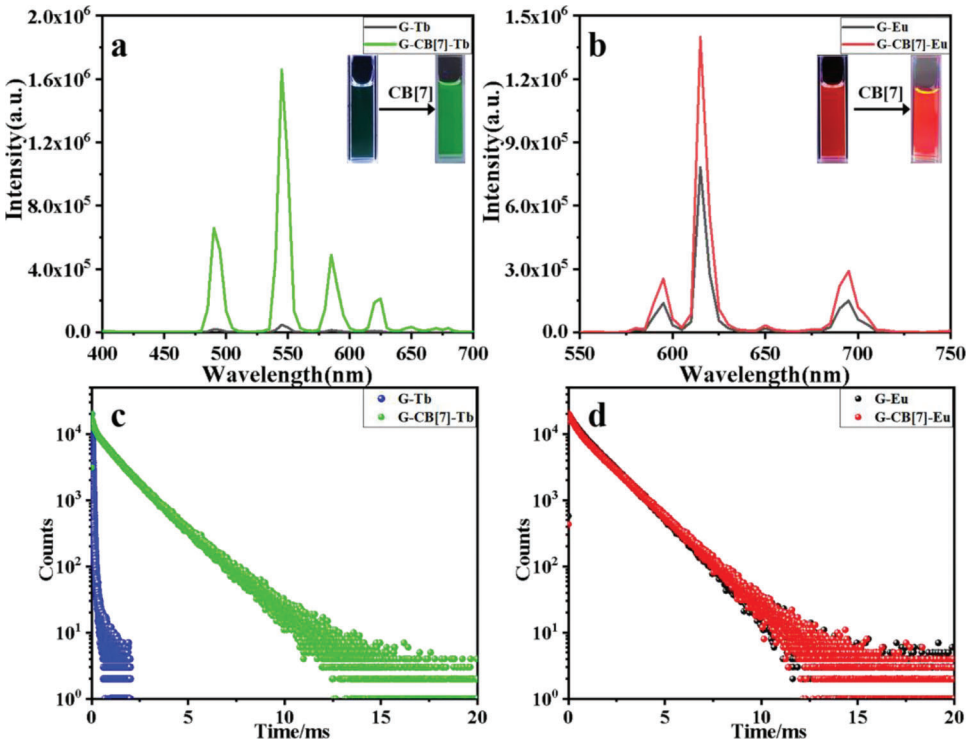

Figure 2. Photoluminescence emission spectra of a) G_1/Tb^{3+} (black line), $CB[7]/G_1/Tb^{3+}$ (green line) and b) G_1/Eu^{3+} (black line), $CB[7]/G_1/Eu^{3+}$ (red line) in H_2O at 298 K. Time-resolved photoluminescence decay curves of c) G_1/Tb^{3+} (blue line), $CB[7]/G_1/Tb^{3+}$ (green line) at 545 nm and d) G_1/Eu^{3+} (black line), $CB[7]/G_1/Eu^{3+}$ (red line) at 615 nm in aqueous solution ($[G_1] = [CB[7]] = 1.0 \times 10^{-5}$ M, $[Tb^{3+}] = [Eu^{3+}] = 0.3 \times 10^{-5}$ M).

formation of complexes and the construction of assemblies increased the surface electronegativity of G_1 (Figure S12, Supporting Information).

Moreover, using this assembly with enhanced lanthanide luminescence, multicolor efficient lanthanide luminescence could be achieved in aqueous solution by adjusting the ratio between red-emitting Eu^{3+} ions and green-emitting Tb^{3+} ions. **Figure 3**a presents the fluorescence spectra of different rare-earth ions (Tb^{3+}/Eu^{3+}) at different ratios, and the corresponding fluorescence of aqueous solution at 254 nm showed that the solution changed from green to yellow to orange to red with corresponding CIE coordinates (Figure 3d) from (0.34, 0.56) to (0.66, 0.33) by increasing proportion of Eu^{3+} in $CB[7]/G_1/Ln$ assembly. Multicolor emissions, especially white light emission, have various applications in solid-state lighting and display media owing to their superior color fidelity and low color distortion.[18] To obtain white light emission, the blue emission specie was introduced into $CB[7]/G_1/Tb^{3+}/Eu^{3+}$ for balancing the red and green luminescence from the lanthanide ions. Carbon dots (CD) as a promising candidate for this purpose because of their distinct blue color emission, superior resistance to photo-bleaching, high water solubility, overall good chemical stability, and low toxicity.[19] Based on the previously reported method, we constructed CD nanoparticles with a size distribution of 4–8 nm (Figure S13, Supporting Information).[20] The zeta potential of CD was −14.4 mV, indicating that there were a large number of carboxylic acid groups on the surface of CD, which was suitable for further co-assembly with positively charged assemblies $CB[7]/G_1/Ln$ (Figure S12, Supporting Information). The absorption and emission of CD were shown in Figure 3b, where a bright pure blue light at about 460 nm could be emitted under the excitation of 254 nm, and this will be beneficial to the realization of the white light system. The assemblies $CB[7]/G_1/Tb^{3+}$, $CB[7]/G_1/Eu^{3+}$, and CD can emit strong green, red, and blue fluorescence, respectively, corresponding to CIE coordinates (0.34, 0.56), (0.66, 0.33) and (0.16, 0.17) in the CIE diagram. Interestingly, with the gradual addition of CD in the yellow luminescent assembly $CB[7]/G_1/Tb^{3+}/Eu^{3+}$ (lanthanide ions ratio $[Tb^{3+}]:[Eu^{3+}] = 2.5:1$), the co-assembly luminescence gradually changed from yellow to white, corresponding to the CIE coordinate of (0.31,0.33), and then to blue. In the lanthanide supramolecular assemblies we constructed, the full-color luminescence could be achieved by adjusting the ratio of Tb^{3+}/Eu^{3+} and CD in water. The TEM displayed the formation of the bulk structure (500 nm) of the co-assembly $CB[7]/G_1/Tb^{3+}/CD$ with an Rh of 687 nm (Figures S10d and S11d, Supporting Information). By comparing the transmittance changes of G_1/Tb^{3+}, $CB[7]/G_1/Tb^{3+}$, and $CB[7]/G_1/Tb^{3+}/CD$ assemblies (Figure S14, Supporting Information), the transmittance of G_1/Tb^{3+}did not change significantly after adding CB[7], but the transmittance at 400 nm decreased sharply after further adding CD. Combined with TEM, DLS, and Zeta potential changes, it can be further proved that CD and $CB[7]/G_1/Tb^{3+}/Eu^{3+}$ are co-assembled. In addition, we investigated the photostability of the assembly, which is very important for luminescent materials. The spectrum of $CB[7]/G_1/Tb^{3+}/Eu^{3+}/CD$ assembly hardly changed after natural light irradiation for 72 h (Figure S15, Supporting Information), indicating that the assembly has satisfactory photostability.

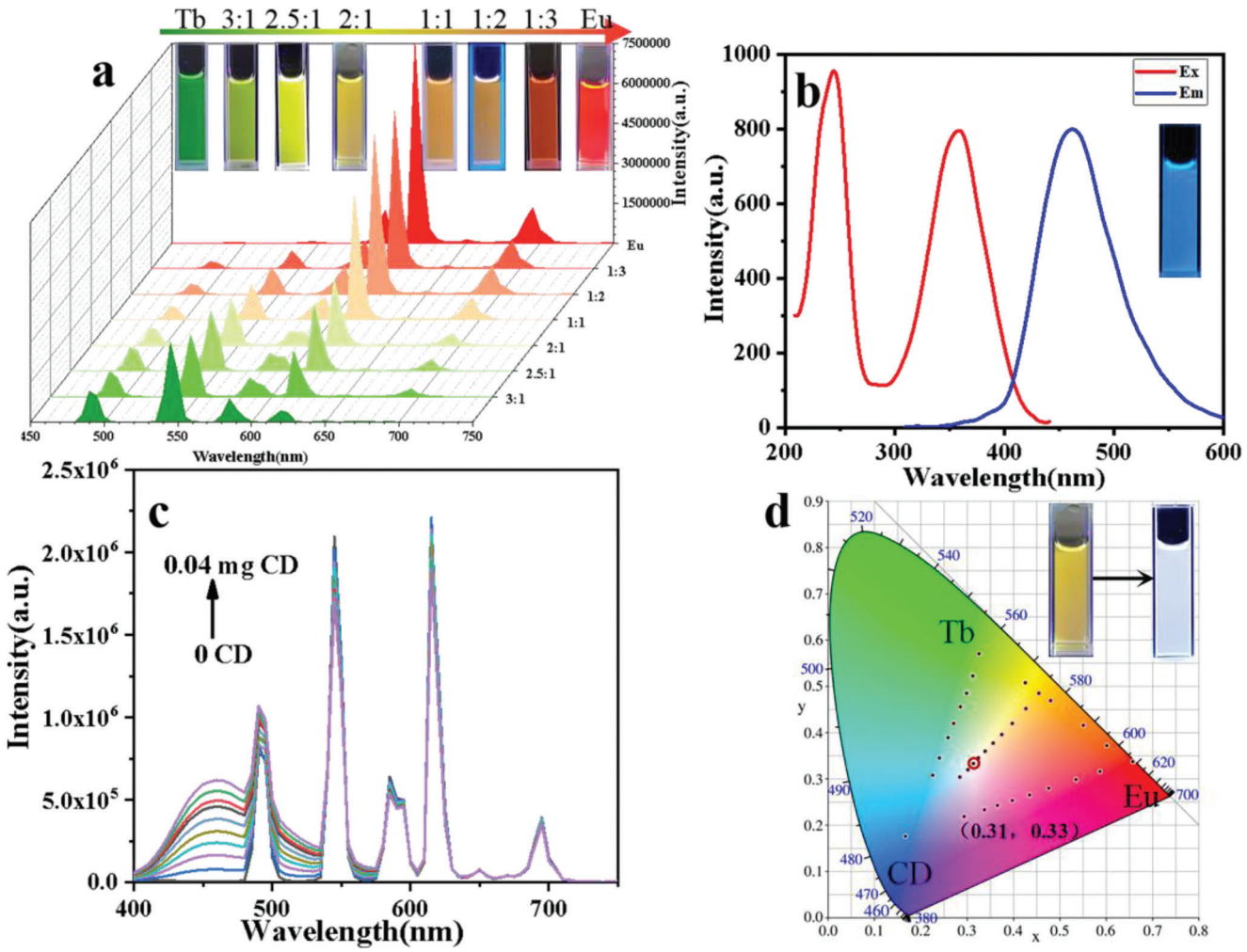

Figure 3. Photoluminescence spectra of different colors a) green, yellow, red with different ratios of Tb^{3+} and Eu^{3+} in CB[7]/G_1/Ln assembly in aqueous solution ([G_1] = CB[7] = 1.0×10^{-5} M, [Ln] = [Tb^{3+}] + [Eu^{3+}] = 0.3×10^{-5} M). Inset: corresponding photographic images of CB[7]/G_1/Ln assemblies under 254 nm UV light; b) Excitation and emission spectra of the anionic CD ([CD] = 10 μg mL^{-1}, 298 K). Inset: corresponding photographic images of CD aqueous solution under 254 nm UV light; c) Photoluminescence spectra of adding CD into CB[7]/G_1/Ln assembly in aqueous solution ([G_1] = CB[7] = 1.0×10^{-5} M, [Ln] = [Tb^{3+}] + [Eu^{3+}] = 0.3×10^{-5} M and [Tb^{3+}]:[Eu^{3+}] = 2.5:1) and d) CIE 1931 chromaticity diagram of corresponding the full-color luminescent coordinates.

ADA has a very large binding constant with CB[7], which is an ideal competitive guest for CB[7] assemblies.[21] The addition of the competitive guest ADA could disassemble the assembly, thereby achieving the regulation of lanthanide luminescence. As shown in Figure S16a, Supporting Information, the photoluminescence intensity of Tb^{3+} was gradually quenched with adding ADA solution to the assembly CB[7]/G_1/Tb^{3+} and showed very weak luminescence until a sufficient amount of ADA solution was added. However, the strong luminescence of G_1/Tb^{3+} was recovered by adding enough CB[7] solution again to form CB[7]/G_1/Tb^{3+} assemblies (Figure S16b, Supporting Information). This process can be cycled at least six times without obvious attenuation as shown in **Figure 4**a, and the same phenomenon can be observed in G_1/Eu^{3+} complexes (Figure 4b, Figure S16c,d, Supporting Information). In order to further prove the confinement effect and the enhancement of the sensitization of CB [7] for the antenna molecule G_1, the promoting effect of other macrocycles, such as COOH-β-cyclodextrin and per-COOH-pillar[5]arene on G_1/Ln were also studied (Figure S17, Supporting Information), where the binding ability of CB[7] with G_1 ($K_a = 9 \times 10^5$ M^{-1}) is much greater than that of the COOH-β-cyclodextrin (about 10^2 M^{-1}) and per-COOH-pillar[5]arene.[22] Thus, no obvious enhancement of optical properties was observed in the reference macrocyclic compound solution. In addition, the protonation of nitrogen and carboxylic acid on pyridine can lead to the dissociation of Ln and DPA under acidic conditions because the DPA is composed of two carboxylic acids and one pyridine.[23] For CB[7]/G_1/Tb^{3+} assemblies (Figure 4c), with increasing the concentration of HCl within a certain range, the photoluminescence spectrum was gradually quenched, while for CB[7]/G_1/Eu^{3+}, the effect was better and almost completely quenched (Figure 4d). The process is reversible by adding sodium hydroxide. In addition to CB[7]/G_1/Tb^{3+}, the luminescence of CB[7]/G_1/Eu^{3+} was also restored from colorless to red, and showed five

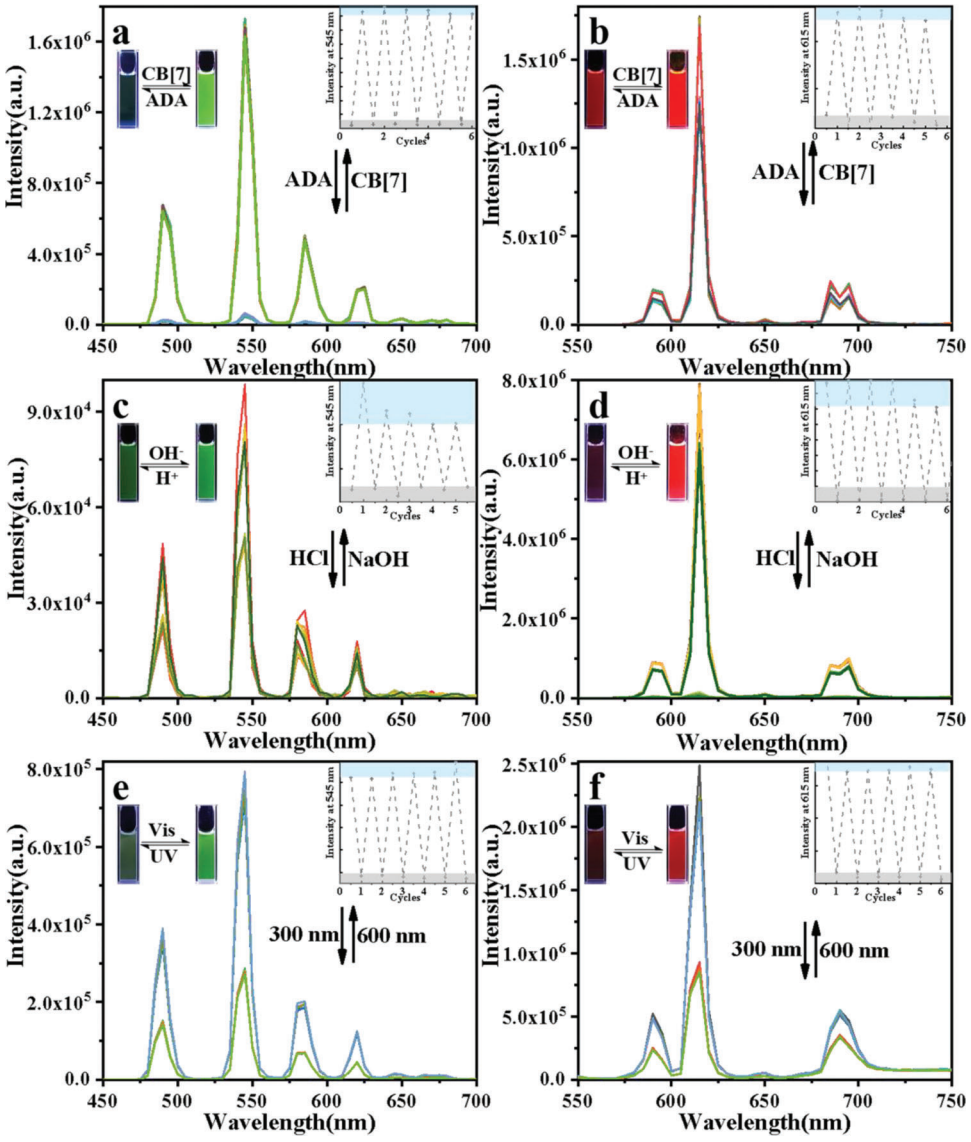

Figure 4. Photoluminescence spectra and emission intensity changes of a) CB[7]/G_1/Tb^{3+} assembly at 545 nm (inset) and b) CB[7]/G_1/Eu^{3+} assembly at 615 nm (inset) upon alternating adding ADA and CB[7] in aqueous solution. Photoluminescence spectra and emission intensity changes of c) CB[7]/G_1/Tb^{3+} assembly at 545 nm (inset) and d) CB[7]/G_1/Eu^{3+} assembly at 615 nm (inset) upon alternating HCl and NaOH in aqueous solution. Photoluminescence spectra and emission intensity changes of e) CB[7]/G_1/Tb^{3+}/DAE assembly at 545 nm (inset) and f) CB[7]/G_1/Eu^{3+}/DAE assembly at 615 nm (inset) upon consecutively alternating exposure to UV and visible light.

better cycles (Figure 4c,d). Additionally, the excellent photoisomerization of DAEs could regulate the ET process with Tb^{3+}/Eu^{3+} luminescence[9,14,24] (Figure S18, Supporting Information). A bispyridinium-modified DAEs with good anti-fatigue properties was introduced into CB[7]/G_1/Ln assemblies (Figure S19, Supporting Information) in which the luminescence of Tb^{3+}/Eu^{3+} ions was well tuned based on the open/closed-ring of DAE under the alternating irradiation of UV/vis light (Figure 4e,f).

More importantly, because the luminescence of Ln in the assembly can be regulated by the competitive encapsulation of ADA and CB[7], the protonation/deprotonation of DPA by H^+/OH^-, and the photoisomerization of DAE, the multi-stimulus response to the panchromatic spectrum of assembly G_1/Ln/CD including white light emission was realized. With the addition of CB[7], the luminescence color of G_1/Ln/CD assembly changed continuously and passes through the white-light region at an appropriate ratio of Eu^{3+}/Tb^{3+}/CD due to the enhanced luminescence of Tb^{3+}/Eu^{3+}, and this process could be reversibly changed by adding ADA, as shown in Figure 5a–c. Subsequently, the protonation and deprotonation of carboxylic acids and nitrogen on pyridines by H^+/OH^- to regulate the coordination of G_1 and Ln could also control the white light emission of CB[7]/G_1/Eu^{3+}/Tb^{3+}/CD (Figure 5d–f). Meanwhile, due to the ET with Ln in the closed-form state and no ET with Ln in the open-form state, doping of DAE derivatives in the assembly CB[7]/G_1/Eu^{3+}/Tb^{3+}/CD also achieved the regulation of white light by alternating UV/vis light irradiation (Figure 5g–i). In view

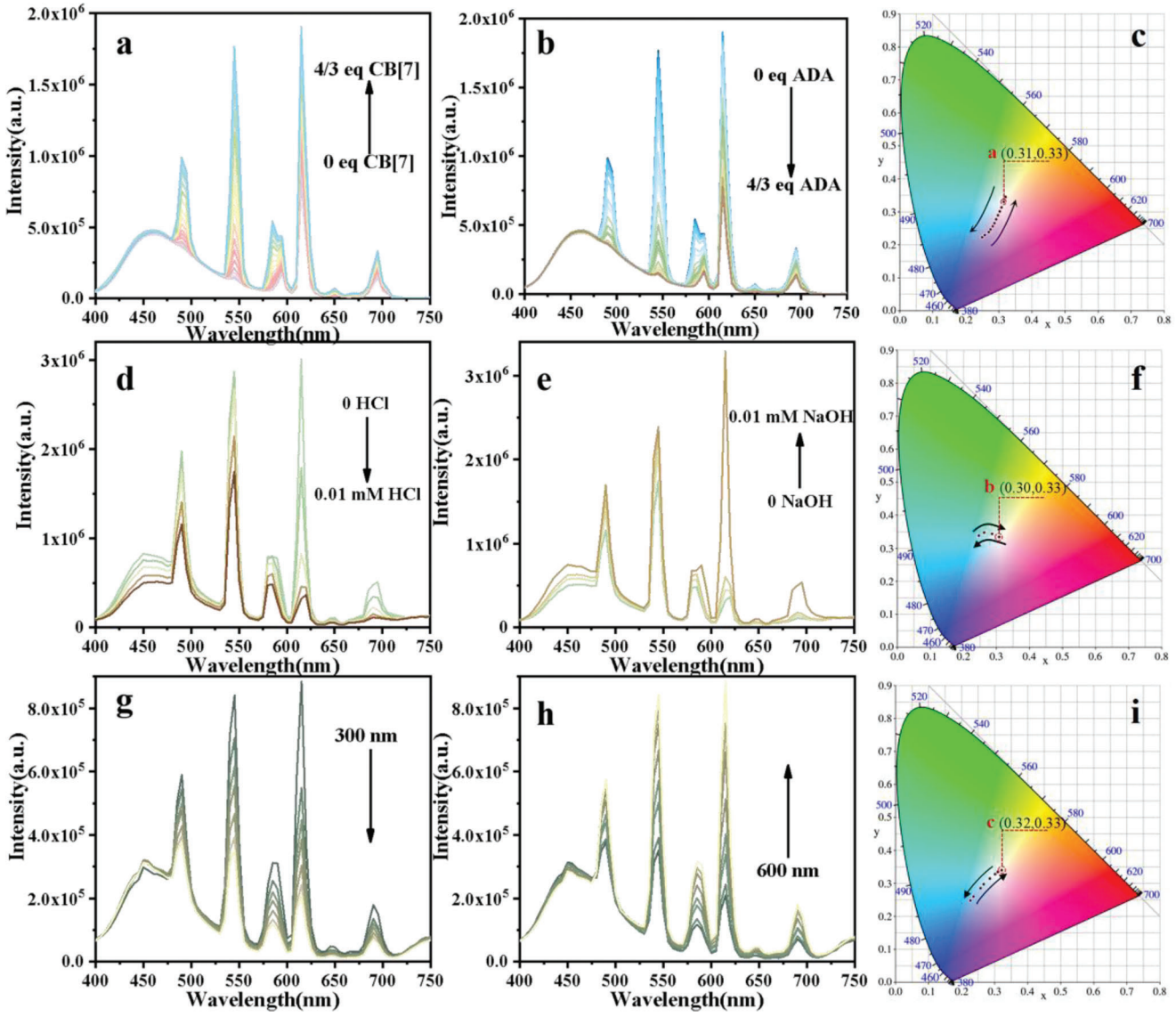

Figure 5. Photoluminescence spectra of a) adding CB[7] and b) adding ADA into $G_1/Tb^{3+}/Eu^{3+}$/CD assembly in aqueous solution, c) corresponding CIE 1931 chromaticity diagram; Photoluminescence spectra of d) adding HCl and e) adding NaOH into CB[7]/$G_1/Tb^{3+}/Eu^{3+}$/CD assembly in aqueous solution, f) corresponding CIE 1931 chromaticity diagram; Photoluminescence spectra of CB[7]/$G_1/Tb^{3+}/Eu^{3+}$/CD/DAE assembly in aqueous solution upon irradiation with g) 300 nm UV light and h) 600 nm vis light for up to 60 s, i) corresponding CIE 1931 chromaticity diagram.

of this satisfactory multi-stimuli-responsive multi-color CB[7]-confined lanthanide supramolecular assembly including white light, it could be applied to construct multiple logic gate anti-counterfeiting systems. The logic device defines different components of the assembly and different stimulus-response elements as input, and white light emission under 254 nm excitation was defined as output (**Figure 6**a). For white light output can be recorded as 1, cannot output is recorded as 0. Therefore, we designed the combinational logic gate systems including three fundamental logic gates for white-light output. The 0 and 1 states of the logic circuit output represent different types of supramolecular assembly. In the logic gate system, the white light emission can be "locked" when CB[7]/G_1/Ln/CD coexists, and the signal can be output in a "silent" manner by using ADA as a NOT gate. At the same time, the CB[7]/G_1/Ln/CD assembly can lock the white light emission with HCl/NaOH inputting into XNOR gate. In addition, the CB[7]/G_1/Ln/CD/DAE_{CF} assembly can output white light after irradiation with 600 nm visible light, so taking 300 nm UV light as a NOT gate, the signal can also be output in a "silent" manner, which were all clearly shown in the truth table. This simple logic gate based on multi-stimuli-responsive lanthanide supramolecular assemblies with white light-emitting can output complex information after adding multiple input components, which provided great potential for the construction of complex logic gate circuits. Furthermore, the multistimuli full-color supramolecular assembly was suitable for multi-level information encryption. The multicolor character "BR" was written by different assembly

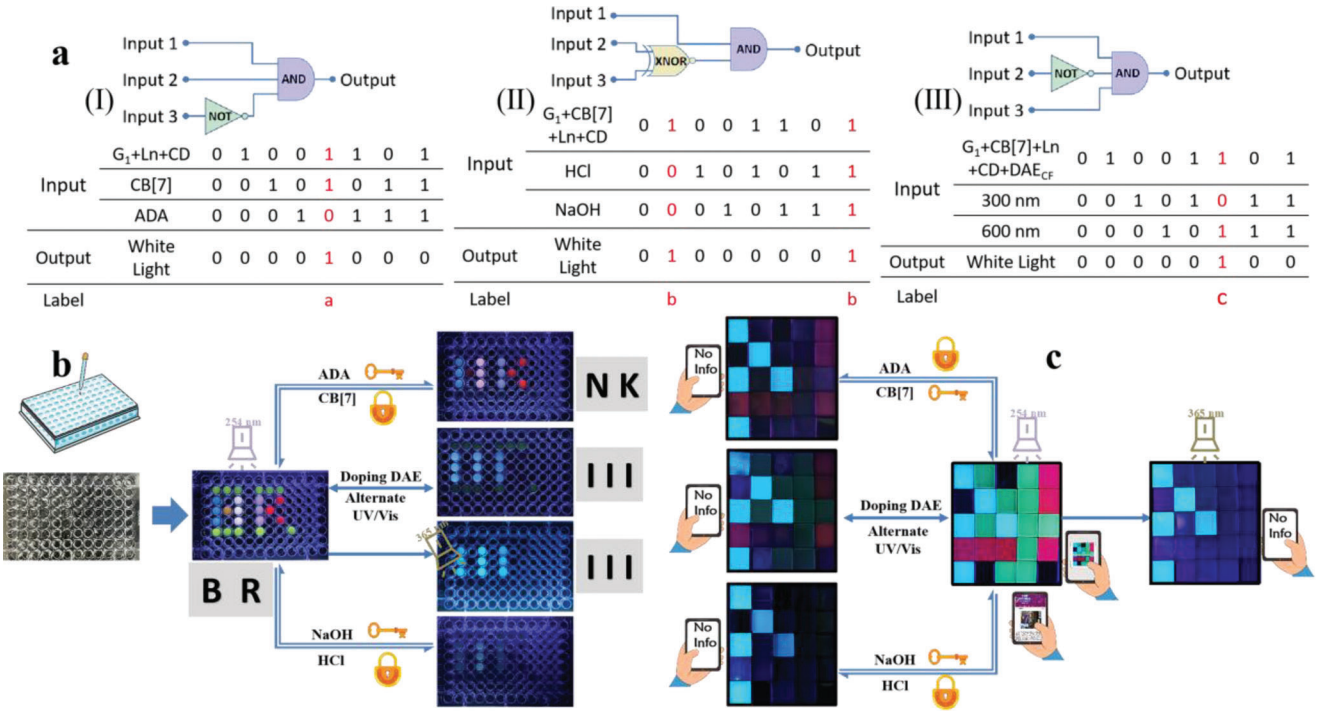

Figure 6. a) Combinational logic gate systems based on luminescent colors of assemblies and the corresponding truth tables. b) Photographs of multi-stimulus-responsive lanthanide supramolecular ink for encryption. c) Photographs of a pattern made up from the assembly of multicolor hydrogel on a black substrate before and after multiple stimulus responsiveness under UV light.

solutions of blue CD, green CB[7]/G_1/Tb^{3+}, red CB[7]/G_1/Eu^{3+}, yellow CB[7]/G_1/Tb^{3+}/Eu^{3+}, purple CB[7]/G_1/Eu^{3+}/CD and white CB[7]/G_1/Tb^{3+}/Eu^{3+}/CD in a porous plate under 254 nm excitation light, as shown in Figure 6b. Interestingly, owing to the multi-stimuli responsiveness of the assembly CB[7]/G_1/Ln, the addition of the competitive guest ADA to the assembly can quench the green luminescence, weaken the red luminescence, and change the multi-color character from "BR" to "NK." Simultaneously, the addition of HCl to the multi-color character "BR" caused the complex to dissociate, the disappearance of green/red luminescence, and the weakening of blue luminescence. Significantly, the character "BR" was doped with DAE solution for the ET with Ln under UV light irradiation, in which green and red similarly disappear, leaving the blue character "111." Due to the excitation wavelength dependence of the luminescence of the assembly (Figure S20, Supporting Information), CD had the maximum excitation wavelength at 360 nm, while the Ln complex was only excited at 254 nm, so the multicolor character "BR" exhibited bright blue digit "111" at 365 nm. These processes were reversible by adding CB[7], NaOH or using vis light irradiation, respectively. On the other hand, using the multicolor tunable luminescence properties of the assembly, the agarose gel was simply dispersed in an aqueous solution with CB[7]/G_1/Ln/CD assemblies to obtain a multicolor luminescent hydrogel (Figure 6c). Furthermore, red-emitting hydrogels (containing Eu^{3+}), green-emitting hydrogels (containing Tb^{3+}), and blue-emitting hydrogels (containing CD) were placed on black substrates, and specific arrangement of colors constructed a luminescence matrix based on three color gel modules (blue CD, green CB [7]/G_1/Tb^{3+}, red CB [7]/G_1/Eu^{3+}) and black background contacting each other which give specific websites as recognition information via a smartphone software APP COLORCODE. Under the sunlight, the hydrogels did not glow, and the information stored in the code cannot be recognized by the application software in the smartphone (Figure S21, Supporting Information). Under the 365 nm UV lamp, the red and green gel blocks did not glow, only the blue module glowed, so the pattern information cannot be recognized. Under the 254 nm UV lamp, the specific luminescence matrix appeared, the software was easy to identify, and the coding information can be read out (Figure 6c, Movie S1, Supporting Information). After dropping ADA, the luminescence of red and green gel blocks was quenched and the luminescence pattern was destroyed. This caused the encoded information to be unreadable and encrypted and the erased pattern can be decrypted and fully recovered by adding CB[7] when needed. In addition, the encryption and decryption of information can also be achieved by dropping HCl and NaOH or changing the excitation wavelength from 254 to 365 nm. Meanwhile, the coding information was modified by doping DAE, and the readability and encryption of the encoding information were realized by alternating irradiation of 600 nm visible light and 300 nm UV light. Then, based on the multi-color fluorescence variation characteristics of the macrocyclic confined lanthanide supramolecular assembly under multi-stimulus response, a multi-level logic gate with encryption characteristics was constructed to store information.

3. Conclusion

In summary, based on the co-assembly of CB[7] and G_1/Ln/CD, we designed and constructed a cucurbit[7]uril-confined tunable

full-color luminescent supramolecular assembly. After CB[7] was added into the G_1/Ln/CD aqueous solution to form a pseudorotaxane complex, the luminescence of G_1/Tb^{3+} was almost from scratch, accompanied by 28-fold increase in quantum yield and 12-fold enhancement in lifetime. The full-color luminescence including white light emission was gained by altering the ratio of Tb^{3+} (green light), Eu^{3+} (red light), and CD (blue light) of the CB[7]/G_1/Ln/CD assembly in this process. Moreover, full-color lanthanide luminescent supramolecular assembly can be intelligently regulated through the competitive encapsulation of host and guest, change of pH, and doping of DAE as well as using different excitation wavelengths. Therefore, the CB[7]-confined full-color lanthanide supramolecular switch with multiple-stimulus response was successfully applied for multi-level logic gate and intelligent multicolor anti-counterfeiting inks, which presents a new opportunity in the design of advanced multifunctional controllable anti-counterfeiting materials.

Supporting Information

Supporting Information is available from the Wiley Online Library or from the author.

Acknowledgements

This work was supported by the National Natural Science Foundation of China (22101143, 22131008, and 21971127), the China Postdoctoral Science Foundation (2021M691661), the National Natural Science Foundation of Inner Mongolia (2021BS02014), the Program for Young Talents of Science and Technology in Universities of Inner Mongolia Autonomous Region (NJYT22050) and the Inner Mongolia Minzu University Doctoral Research Fund (BS554).

Conflict of Interest

The authors declare no conflict of interest.

Author Contributions

W.-L.Z. and W.L. contributed equally to this work. Y.C. and Y.L. conceived and designed the experiments. W.-L.Z. and X.-Y.D. synthesized and performed the chemical characterization. W.L. performed anti-counterfeiting applications and drawings. W.-L.Z. and W.L. wrote the main manuscript. Y.L. supervised the work and edited the manuscript. All authors analyzed and discussed the results and reviewed the manuscript.

Data Availability Statement

The data that support the findings of this study are available from the corresponding author upon reasonable request.

Keywords

cucurbit[7]uril-confined, lanthanide luminescence, supramolecular assemblies, tunable multicolored, white light emission

Received: May 12, 2023
Revised: June 21, 2023
Published online:

[1] a) X. Z. Li, C. B. Tian, Q. F. Sun, *Chem. Rev.* **2022**, *122*, 6374; b) O. Kotova, C. O'Reilly, S. T. Barwich, L. E. Mackenzie, A. D. Lynes, A. J. Savyasachi, M. Ruether, R. Pal, M. E. Möbius, T. Gunnlaugsson, *Chem* **2022**, *8*, 1395; c) M. Isaac, S. A. Denisov, A. Roux, D. Imbert, G. Jonusauskas, N. D. McClenaghan, O. Seneque, *Angew. Chem., Int. Ed.* **2015**, *54*, 11453; d) E. G. Moore, A. P. S. Samuel, K. N. Raymond, *Acc. Chem. Res.* **2009**, *42*, 542.
[2] L. Jullien, J. Canceill, B. Valeur, E. Bardez, J.-P. Lefèvre, J.-M. Lehn, V. Marchi-Artzner, R. Pansu, *J. Am. Chem. Soc.* **1996**, *118*, 5432.
[3] a) T. M. Ajayi, V. Singh, K. Z. Latt, S. Sarkar, X. Cheng, S. Premarathna, N. K. Dandu, S. Wang, F. Movahedifar, S. Wieghold, N. Shirato, V. Rose, L. A. Curtiss, A. T. Ngo, E. Masson, S. W. Hla, *Nat. Commun.* **2022**, *13*, 6305; b) W. L. Chan, C. Xie, W. S. Lo, J. G. Bunzli, W. K. Wong, K. L. Wong, *Chem. Soc. Rev.* **2021**, *50*, 12189; c) L. Wang, Z. Zhao, C. Wei, H. Wei, Z. Liu, Z. Bian, C. Huang, *Adv. Opt. Mater.* **2019**, *7*, 1801256; d) R. Emmanuele, M. Maciejczyk, A. Smith, X. Cheng, E. Masson, D. J. Gosztola, S. W. Hla, N. Robertson, X. Ma, *ACS Photonics* **2022**, *9*, 2315.
[4] a) J. F. Lemonnier, L. Babel, L. Guenee, P. Mukherjee, D. H. Waldeck, S. V. Eliseeva, S. Petoud, C. Piguet, *Angew. Chem., Int. Ed.* **2012**, *51*, 11302; b) G. Zhan, L. Wang, Z. Zhao, P. Fang, Z. Bian, Z. Liu, *Angew. Chem., Int. Ed.* **2020**, *59*, 19011.
[5] a) Y. Yang, Y. Liu, D. Tu, M. Chen, Y. Zhang, H. Gao, X. Chen, *Angew. Chem., Int. Ed.* **2022**, *61*, e202116983; b) Z. Yi, Z. Luo, X. Qin, Q. Chen, X. Liu, *Acc. Chem. Res.* **2020**, *53*, 2692; c) G. Q. Jin, C. V. Chau, J. F. Arambula, S. Gao, J. L. Sessler, J. L. Zhang, *Chem. Soc. Rev.* **2022**, *51*, 6177; d) J. Yan, B. Li, P. Yang, J. Lin, Y. Dai, *Adv. Funct. Mater.* **2021**, *31*, 2104325.
[6] a) T. Yimyai, T. Phakkeeree, D. Crespy, *Adv. Sci.* **2020**, *7*, 1903785; b) Z. Li, H. Chen, B. Li, Y. Xie, X. Gong, X. Liu, H. Li, Y. Zhao, *Adv. Sci.* **2019**, *6*, 1901529; c) X. Xu, J. Wang, B. Yan, *Adv. Funct. Mater.* **2021**, *31*, 2103321; d) G. Weng, S. Thanneeru, J. He, *Adv. Mater.* **2018**, *30*, 1706526; e) B. Li, Z.-J. Ding, Z. Li, H. Li, *J. Mater. Chem. C* **2018**, *6*, 6869.
[7] a) T. Song, G. Zhang, Y. Cui, Y. Yang, G. Qian, *CrystEngComm* **2016**, *18*, 8366; b) D. A. Galico, A. A. Kitos, J. S. Ovens, F. A. Sigoli, M. Murugesu, *Angew. Chem., Int. Ed.* **2021**, *60*, 6130; c) S. Mund, S. Vaidyanathan, *J. Mater. Chem. C* **2022**, *10*, 7201; d) Q. Zhu, L. Zhang, K. Van Vliet, A. Miserez, N. Holten-Andersen, *ACS Appl. Mater. Interfaces* **2018**, *10*, 10409.
[8] P. Chen, Q. Li, S. Grindy, N. Holten-Andersen, *J. Am. Chem. Soc.* **2015**, *137*, 11590.
[9] Z. Li, X. Liu, G. Wang, B. Li, H. Chen, H. Li, Y. Zhao, *Nat. Commun.* **2021**, *12*, 1363.
[10] R. Wang, Y. Zhang, W. Lu, B. Wu, S. Wei, S. Wu, W. Wang, T. Chen, *Angew. Chem., Int. Ed.* **2023**, *62*, e202300417.
[11] a) W.-L. Zhou, Y. Chen, W. Lin, Y. Liu, *Chem. Commun.* **2021**, *57*, 11443; b) W.-L. Zhou, Y. Chen, Y. Liu, *Acta Chim. Sin.* **2020**, *78*, 1164; c) W. Zhou, Y. Chen, Q. Yu, P. Li, X. Chen, Y. Liu, *Chem. Sci.* **2019**, *10*, 3346; d) W.-L. Zhou, X.-Y. Dai, W. Lin, Y. Chen, Y. Liu, *Chem. Sci.* **2023**, *14*, 6457.
[12] H. Yao, X.-T. Kan, Q. Zhou, Y.-B. Niu, Y.-M. Zhang, T.-B. Wei, Q. Lin, *ACS Sustainable Chem. Eng.* **2020**, *8*, 13048.
[13] a) Z. Li, G. Wang, Y. Wang, H. Li, *Angew. Chem., Int. Ed.* **2018**, *57*, 2194; b) H. J. Yu, H. Wang, F. F. Shen, F. Q. Li, Y. M. Zhang, X. Xu, Y. Liu, *Small* **2022**, *18*, 2201737.
[14] H. B. Cheng, H. Y. Zhang, Y. Liu, *J. Am. Chem. Soc.* **2013**, *135*, 10190.
[15] Y. Zhou, H. Y. Zhang, Z. Y. Zhang, Y. Liu, *J. Am. Chem. Soc.* **2017**, *139*, 7168.
[16] a) W. L. Zhou, Y. Chen, Q. Yu, H. Zhang, Z. X. Liu, X. Y. Dai, J. J. Li, Y. Liu, *Nat. Commun.* **2020**, *11*, 4655; b) W.-L. Zhou, W. Lin, Y. Chen, Y. Liu, *Chem. Sci.* **2022**, *13*, 7976.
[17] W. Zhou, Y. Chen, X. Dai, H. Y. Zhang, Y. Liu, *Org. Lett.* **2019**, *21*, 9363.

[18] a) E. Jang, S. Jun, H. Jang, J. Lim, B. Kim, Y. Kim, *Adv. Mater.* **2010**, *22*, 3076; b) Z. Zhang, Y. Chen, H. Chang, Y. Wang, X. Li, X. Zhu, *J. Mater. Chem. C* **2020**, *8*, 2205.
[19] a) S. Zhu, Q. Meng, L. Wang, J. Zhang, Y. Song, H. Jin, K. Zhang, H. Sun, H. Wang, B. Yang, *Angew. Chem., Int. Ed.* **2013**, *52*, 3953; b) S. Y. Lim, W. Shen, Z. Gao, *Chem. Soc. Rev.* **2015**, *44*, 362.
[20] H. Wu, Y. Chen, X. Dai, P. Li, J. F. Stoddart, Y. Liu, *J. Am. Chem. Soc.* **2019**, *141*, 6583.
[21] T. Jiang, G. Qu, J. Wang, X. Ma, H. Tian, *Chem. Sci.* **2020**, *11*, 3531.
[22] a) H. Sanyo, *Bull. Chem. Soc. Jpn.* **1986**, *59*, 2979; b) A. Ponce, P. A. Wong, J. J. Way, D. G. Nocera, *J. Phys. Chem.* **1993**, *97*, 11137; c) N. Song, T. Kakuta, T. Yamagishi, Y.-W. Yang, T. Ogoshi, *Chem* **2018**, *4*, 2029; d) M. Xue, Y. Yang, X. Chi, Z. Zhang, F. Huang, *Acc. Chem. Res.* **2012**, *45*, 1294.
[23] X. Zhou, L. Wang, Z. Wei, G. Weng, J. He, *Adv. Funct. Mater.* **2019**, *29*, 1903543.
[24] J. J. Li, H. Y. Zhang, G. Liu, X. Dai, L. Chen, Y. Liu, *Adv. Opt. Mater.* **2021**, *9*, 2001702.